A UNITED STATES
DEPARTMENT OF
COMMERCE
PUBLICATION

# NOAA Technical Report NOS 59

U.S. DEPARTMENT OF COMMERCE
National Oceanic and Atmospheric Administration
National Ocean Survey

# Gravity Gradients at Satellite Altitudes

B. CHOVITZ
J. LUCAS
F. MORRISON

ROCKVILLE, MD.
November 1973

## NOAA TECHNICAL REPORTS

### National Ocean Survey Series

The National Ocean Survey (NOS) provides charts and related information for the safe navigation of marine and air commerce. The survey also furnishes other earth science data—from geodetic hydrographic, oceanographic, geomagnetic, seismologic, gravimetric, and astronomic surveys, observations, investigations, and measurements—to protect life and property and to meet the needs of engineering, scientific, defense, commercial, and industrial interests.

Because many of these reports deal with new practices and techniques, the views expressed are those of the authors and do not necessarily represent final survey policy. NOS series NOAA Technical Reports is a continuation of, and retains the consecutive numbering sequence of, the former series, Environmental Science Services Administration (ESSA) Technical Reports Coast and Geodetic Survey (C&GS), and the earlier series, C&GS Technical Bulletins.

Those publications marked by an asterisk are out of print. The others are available through the Superintendent of Documents, U.S. Government Printing Office, Washington, D.C. 20402. Price as indicated. Beginning with 39, microfiche is available at the National Technical Information Service (NTIS), U.S. Department of Commerce, Sills Bldg., 5285 Port Royal Road, Springfield, Va. 22151. Price $1.45. Order by accession number, when given, in parentheses.

### COAST AND GEODETIC SURVEY TECHNICAL BULLETINS

*No. 22 Tidal Current Surveys by Photogrammetric Methods. Morton Keller, October 1963.

*No. 23 Aerotriangulation Strip Adjustment. M. Keller and G. C. Tewinkel, August 1964.

*No. 24 Satellite Triangulation in the Coast and Geodetic Survey. February 1965.

*No. 25 Aerotriangulation: Image Coordinate Refinement. M. Keller and G. C. Tewinkel, March 1965.

*No. 26 Instrumented Telemetering Deep Sea Buoys. H. W. Straub, J. M. Arthaber, A. L. Copeland, and D. T. Theodore, June 1965.

*No. 27 Survey of the Boundary Between Arizona and California. Lansing G. Simmons, August 1965.

*No. 28 Marine Geology of the Northeastern Gulf of Maine. R. J. Malloy and R. N. Harbison, February 1966.

*No. 29 Three-Photo Aerotriangulation. M. Keller and G. C. Tewinkel, February 1966.

*No. 30 Cable Length Determinations for Deep-Sea Oceanographic Operations. Robert C. Darling, June 1966.

*No. 31 The Automatic Standard Magnetic Observatory. L. R. Aldredge and I. Saldukas, June 1966.

### ESSA TECHNICAL REPORTS

*C&GS 32 Space Resection in Photogrammetry. M. Keller and G. C. Tewinkel, September 1966.

*C&GS 33 The Tsunami of March 28, 1964, as Recorded at Tide Stations. M. G. Spaeth and S. C. Berkman, July 1967.

*C&GS 34 Aerotriangulation: Transformation of Surveying and Mapping Coordinate Systems. Melvin J. Umbach, August 1967.

*C&GS 35 Block Analytic Aerotriangulation. M. Keller and G. C. Tewinkel, November 1967.

*C&GS 36 Geodetic and Grid Angles—State Coordinate Systems. Lansing G. Simmons, January 1968.

*C&GS 37 Precise Echo Sounding in Deep Water. George A. Maul, January 1969.

*C&GS 38 Grid Values of Total Magnetic Intensity IGRF—1965. E. B. Fabiano and N. W. Peddie, April 1969.

C&GS 39 An Advantageous, Alternative Parameferization of Rotations for Analytical Photogrammetry. Allen J. Pope, September 1970. Price $0.30 (COM-71-00077)

C&GS 40 A Comparison of Methods for Computing Gravitational Potential Derivatives. L. J. Gulick, September 1970. Price $0.40 (COM-71-00185)

(Continued on inside back cover)

U.S. DEPARTMENT OF COMMERCE
Frederick B. Dent, Secretary

NATIONAL OCEANIC AND ATMOSPHERIC ADMINISTRATION
Robert M. White, Administrator

NATIONAL OCEAN SURVEY
Allen L. Powell, Director

NOAA Technical Report NOS 59

# Gravity Gradients at Satellite Altitudes

B. Chovitz
J. Lucas
F. Morrison

ROCKVILLE, MD.
NOVEMBER 1973

For sale by the Superintendent of Documents, U.S. Government Printing Office
Washington, D.C. 20402 - Price 55 cents
Stock Number 0317-00154

UDC 528.271:629.783:517.51/.52

| | |
|---|---|
| 517 | Mathematical analysis |
| .51 | Functions of real variables |
| .52 | Harmonic analysis of infinite series |
| 528 | Geodesy |
| .271 | Gravity anomaly measurement |
| 629 | Aeronautics and astronautics |
| .783 | Artificial earth satellites |

# Contents


| | Page |
|---|---|
| Abstract | 1 |
| 1. Gravity anomalies to spherical harmonics | 3 |
| 2. Spherical harmonics to gravity gradients | 4 |
| 3. Simple averaging of results | 7 |
| 4. Harmonic analysis of results | 10 |
| Acknowledgments | 17 |
| References | 17 |
| Tables | 19 |

# Gravity Gradients at Satellite Altitudes

B. CHOVITZ, J. LUCAS, F. MORRISON

*Geodetic Research and Development Laboratory*
*National Geodetic Survey*

ABSTRACT. The availability of detailed worldwide gravity anomaly information in the form of 1° square blocks makes possible the computation of gravity gradients at close (under 300 km) altitudes, thus indicating the sensitivity required of a satellite-borne gradiometer. As a first step, the gravity anomaly data are transformed to spherical harmonics up to degree and order 75. A comparison with the global rule-of-thumb, $10^{-5}/l^2$, for the r.m.s. magnitude of an individual normalized harmonic of degree $l$ shows close agreement for $15 \leq l \leq 75$. Satellite orbits are then generated by numerical integration, the time step being set to a sampling rate of the gradiometer, and gravity gradients can be computed at this interval. A coordinate system is chosen to correspond to the axis of rotation of the instrument.

Results of simple averaging indicate that to distinguish the combined harmonics of a single degree in the range of 60 or 70, a sensitivity of better than 0.01 Eötvös unit is required, and to pick up the total band of harmonics between degrees 60 and 70, a sensitivity of 0.02 Eötvös unit is needed. However, a detailed harmonic analysis making use of the maximum entropy technique shows that specific components of degree around 70 with amplitude higher than 0.03 Eötvös unit can be distinguished. A gradiometer sensitive to 0.01 Eötvös unit therefore should provide useful information.

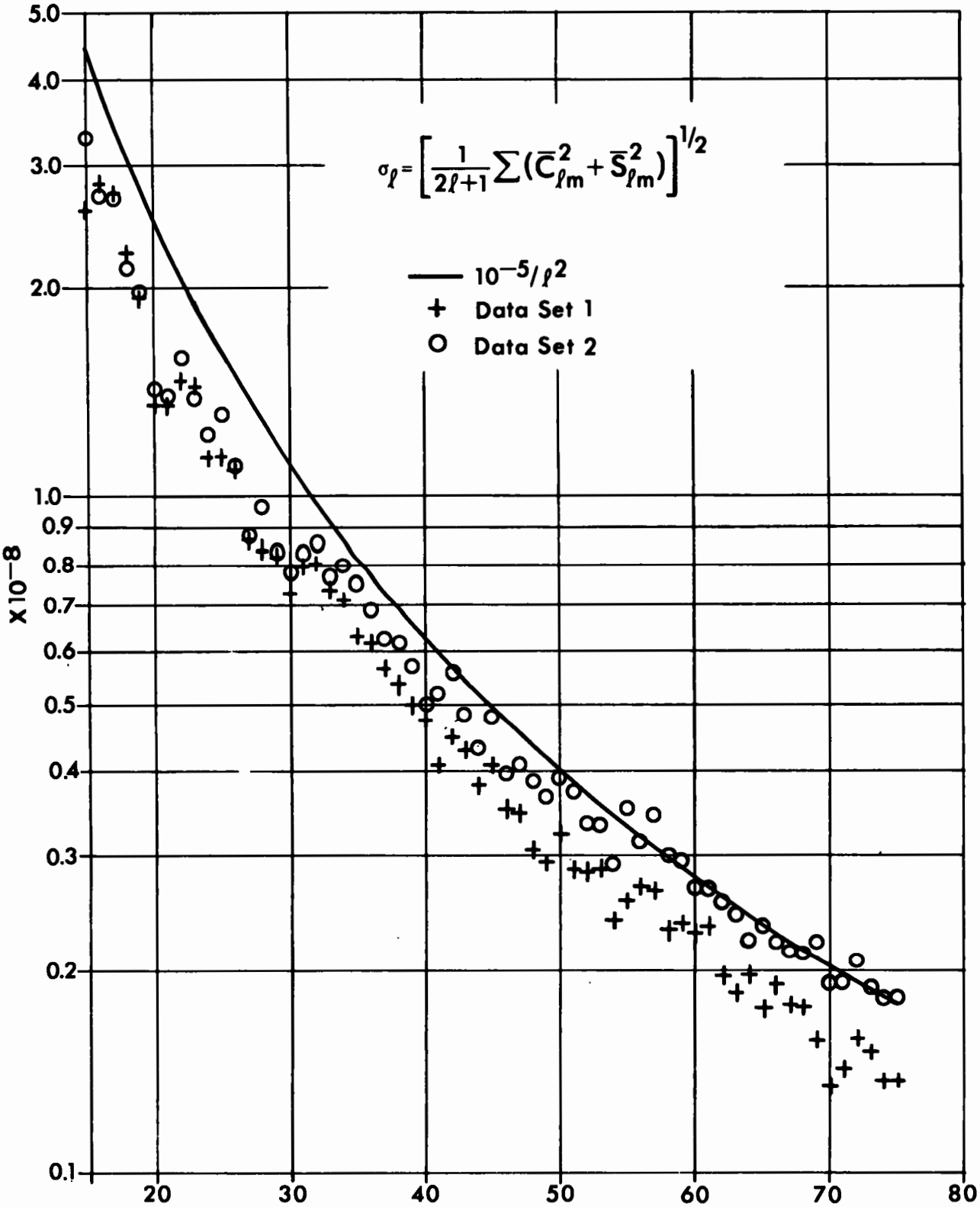


FIGURE 1.—*Comparison of two sets of discrete degree variances, $\sigma_l$, $(15 \leq l \leq 75)$ computed from observed data against the rule-of-thumb $10^{-5}/l^2$.*

## 1. GRAVITY ANOMALIES TO SPHERICAL HARMONICS

Among the various methods being considered for improving knowledge of the global gravity field by satellites, gravity gradiometry is one of the most promising (Kaula 1969). Its advantages are independence of tracking stations and other satellites, near-continuous data gathering, and sensitivity to the higher harmonics of the field. However, it requires a dedicated satellite and an instrument whose precision appears to strain the limit of current technological capabilities.

The purpose of this study is to determine the magnitude of gravity gradients at low satellite altitudes (about 300 km) so that the sensitivity level required of a satellite gradiometer instrument can be ascertained. Previous quantitative analyses of this nature (Kaula 1971, Forward 1972) were based essentially on Kaula's rule-of-thumb, which expresses the magnitude of the individual normalized harmonic coefficient of degree $l$ as $10^{-5}/l^2$. Other empirical rules of this nature, e.g., by Meissl (1971), differ very little in substance. For the effect of all harmonics of degree $l$, Kaula (1971) estimated about $10^{-2}$ EU (Eötvös unit$-1$ Eötvös unit$=10^{-9}$ gal/cm) for $l=40$, and $0.5\times10^{-2}$ EU for $l=75$ at 260-km altitude. Forward's (1972) figures are roughly twice those of Kaula, because of a different method of summation and a slight variation in the power law.

The solid line in figure 1 depicts the (nondimensional) magnitude of the set of normalized spherical harmonics of degree $l$ according to Kaula's rule-of-thumb.

The above estimates are global averages based on an empirical rule from which wide deviations possibly could occur in specific areas. We first utilized a published (Aeronautical Chart and Information Center 1971) set of approximately 20,000 $1^\circ\times1^\circ$ gravity anomalies based on observed data, covering about 30 percent of the world. Subsequently we obtained several thousand additional $1^\circ\times1^\circ$ anomalies, which increased the coverage considerably. Although the quality of material is variable, coverage over certain land areas, such as the United States and Europe, is quite dense and accurate. It could, therefore, be considered that the field is sufficiently known over these specific regions so that gravity gradient values at altitude could be judged to assume their actual values and vary as a function of position.

Because a satellite-borne gradiometer would sample the field approximately every 30 seconds along the path of a satellite orbit, our approach was to simulate typical satellite orbits over areas of dense coverage, and compute from the data gravity gradients at discrete intervals along the path. Orbital procedures previously programmed in the Geodetic Research and Development Laboratory (Gulick 1970, Witte 1971), which already included the computations of exactly those quantities desired, could be used with little or no alteration if the gravitational field were expressed in terms of spherical harmonics.

Therefore, the first step in the computation was the conversion of the set of gravity anomalies $\Delta g$ to spherical harmonics of degree $l$ and order $m$ by the standard formula

$$\begin{Bmatrix}\bar{C}_{lm}\\ \bar{S}_{lm}\end{Bmatrix}=\frac{a}{4\pi\mu(l-1)}\int_\Sigma\int\Delta g\,\bar{P}_{lm}(\sin\phi)\begin{Bmatrix}\cos m\lambda\\ \sin m\lambda\end{Bmatrix}d\Sigma,$$

where the overbar indicates that the spherical harmonic coefficients $C_{lm}$, $S_{lm}$ and Legendre polynomials $P_{lm}$ are normalized; $\phi$ and $\lambda$ are geocentric latitude and longitude, $a$ is the Earth's semi-major axis, and $\mu$ is the Newtonian gravitational constant times the Earth's mass.

But this requires integration over the entire surface, $\Sigma$, of the Earth, and there were gaps in the sets of $1^\circ\times1^\circ$ anomalies. A set of $5^\circ\times5^\circ$ mean anomalies obtained from Air Force Cambridge Research Laboratories was used to fill these gaps. The equation was then computed in the following manner: The integration was replaced by a summation over $1^\circ$ squares for the entire globe. If $\Delta g$ was available for a given $1^\circ$ square from the $1^\circ$ set, it was used; otherwise $\Delta g$ was assigned the value of the $5^\circ$ square in which it fell. The computation was carried out through $l$, $m=88$. However, the series could be applied usefully only through 75th degree and order, since numerical problems caused the magnitudes of the coefficients to diverge upward beyond this point. For this study, it was judged that the series through 75th degree was sufficient, so no attempt has been made to isolate and correct the cause of this divergence.

In figure 1 the set of discrete points plot

$$\sigma_l=\frac{1}{2l+1}\sum_m\left[(\bar{C}_{lm}^2+\bar{S}_{lm}^2)\right]^{1/2}.$$

The crosses and circles designate the values based on the smaller and larger sets of 1° anomalies, respectively. The lesser set yielded magnitudes about 25 percent less than the $10^{-5}/l^2$ curve, but this deficiency is almost completely eliminated by the larger set. This is an excellent confirmation of Kaula's rule-of-thumb. The discrepancy of the smaller set probably is due to artificial smoothing introduced by the more extensive use of the 5° anomalies.

## 2. SPHERICAL HARMONICS TO GRAVITY GRADIENTS

At this point we have available a set of spherical harmonics up to degree and order 75 with which to calculate the gradients of gravity at any external point we choose. Since a gradiometer will sample the field at a given rate (about 30 seconds) along an orbit about 300 km high, we simulated such orbits, choosing paths that traversed over areas of dense 1°×1° anomaly coverage. The satellite orbit is generated by a numerical integration program in which the time steps of the integration are set to the sampling rate of the gradiometer. A position is calculated for each sampling time, and the six distinct gravity gradient components are computed as a function of position.

Gravity gradients are conveniently defined and manipulated by tensor formalism. The gravity gradient is the second covariant derivative of the potential, which for a Cartesian coordinate system is the matrix of second partials of the potential $N$,

$$N_{qs} = (\partial^2 N/\partial x^q \partial x^s).$$

This matrix is symmetric, and since Laplace's equation holds it has but *five* independent quantities. Laplace's equation

$$\nabla^2 N = 0$$

may also be written

$$\text{Trace}\,(N_{qs}) = 0.$$

The reward in using the tensor formalism is that equations and definitions are easily transformed to another coordinate system indicated by an * (asterisk) in the following equations:

$$N^*_{ut} = J^q_u J^s_t N_{qs}$$

$$J^q_u = \frac{\partial x^q}{\partial x^{*u}}$$

In matrix notation this is

$$N^* = J' N J'^T,$$

where $J'$ is the inverse of the Jacobian matrix. Derivations of these formulas and others are given by Hotine (1969), who named the gravity gradient the "Marussi tensor."

Comparisons are made along the same trajectory between gradients obtained from spherical harmonic geopotential models truncated at both low and high degrees. The differences between the gravity gradients will provide an indication of the contribution made to the gravity gradient by the higher degree harmonics.

All the orbit computations are done in an inertial coordinate system. The components of $N_{qs}$ may be printed out in the inertial system, or it may be transformed into either of two other coordinate systems:

A. The "Gravity" Coordinate System

The 3-axis is defined by the local vertical, i.e.,

$$\hat{\mathbf{k}} = -\mathbf{g}/g,$$

where $\mathbf{g}$ is the force of gravity expressed as a vector, and $g$ its magnitude. Then the 2-axis is defined by the projection of the satellite's velocity vector, $\dot{\mathbf{r}}$, onto the 1–2 plane (fig. 2).

B. The "Orbital" Coordinate System

The 3-axis is defined as before, but the 2-axis is defined by the intersection of the orbital plane with the 1–2 plane (fig. 3). Note that the orbital plane is defined by the angular momentum vector

$$\mathbf{h} = \mathbf{r} \times \dot{\mathbf{r}}.$$

For the "gravity" or "orbital" coordinate systems the gradient takes on a highly diagonal form. If only the central force field were present ($N = \mu/r$), for these coordinate systems, $x = y = 0$, $z = r$. Then

$$N^*_{qs} = \begin{bmatrix} -\mu/r^3 & 0 & 0 \\ 0 & -\mu/r^3 & 0 \\ 0 & 0 & 2\mu/r^3 \end{bmatrix}$$

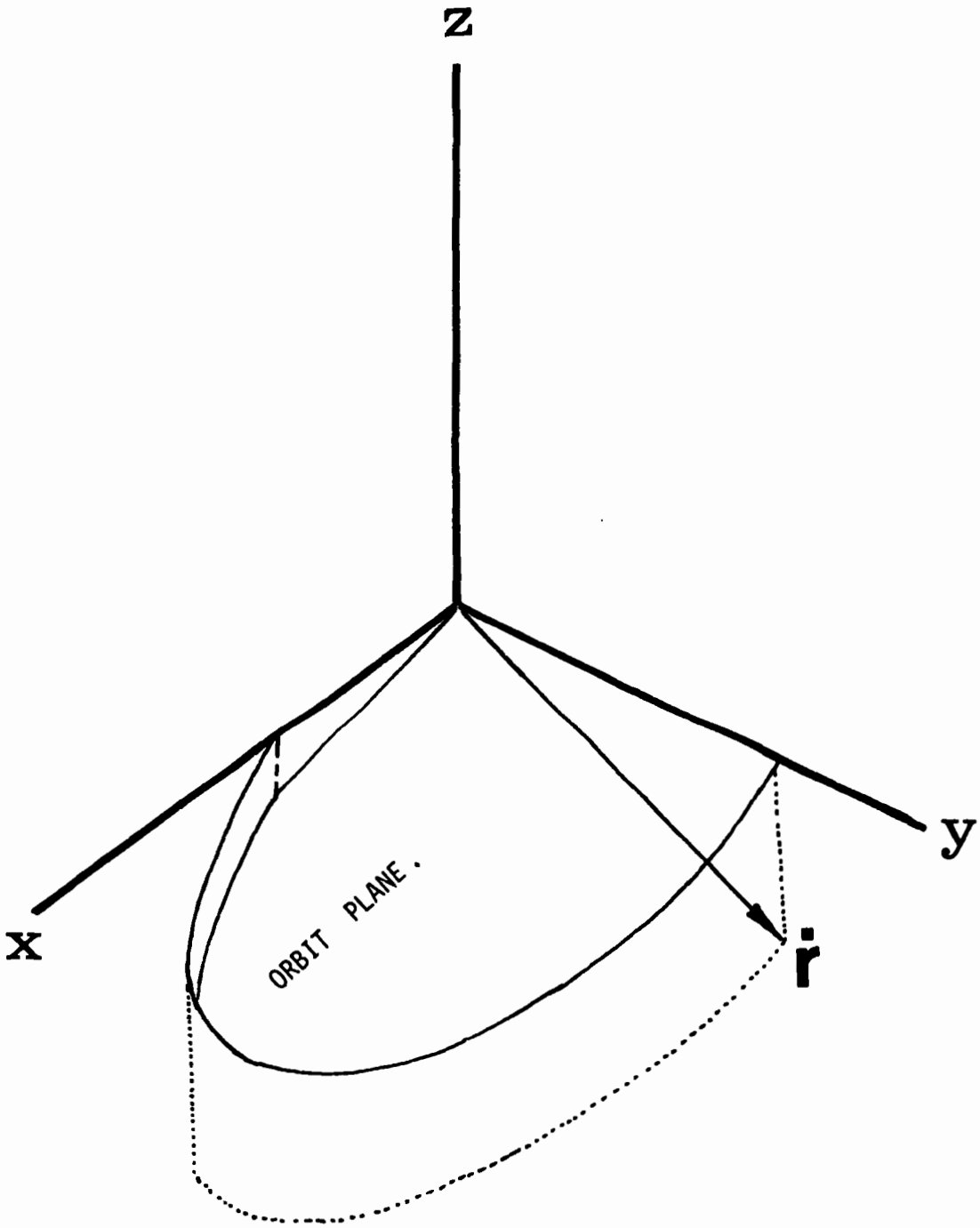


FIGURE 2.—*The "gravity" coordinate system.*

For a more realistic gravity model, the off diagonal terms are of the order of the oblateness, but the diagonal terms sum to zero by Laplace's equation.

Direct comparison can be made between gradients computed for the same time and nearly same trajectory. However, the comparison can be made more effectively by doing a harmonic analysis of the gradients. The differences between gravity gradients derived from high and low degree fields should be in the higher frequencies. For a close satellite, the ground track is about 7.3 km/s, which, for a resolution of 250 to 1,200 km, implies that the wavelengths of interest will be about 30 to 180 seconds. For an integration time step of 30 seconds, this indicates a range of 1 to 6 time steps.

In choosing runs for the determination of gravity gradients, our purpose was twofold: first, to vary the gravitational model by selection of maximum

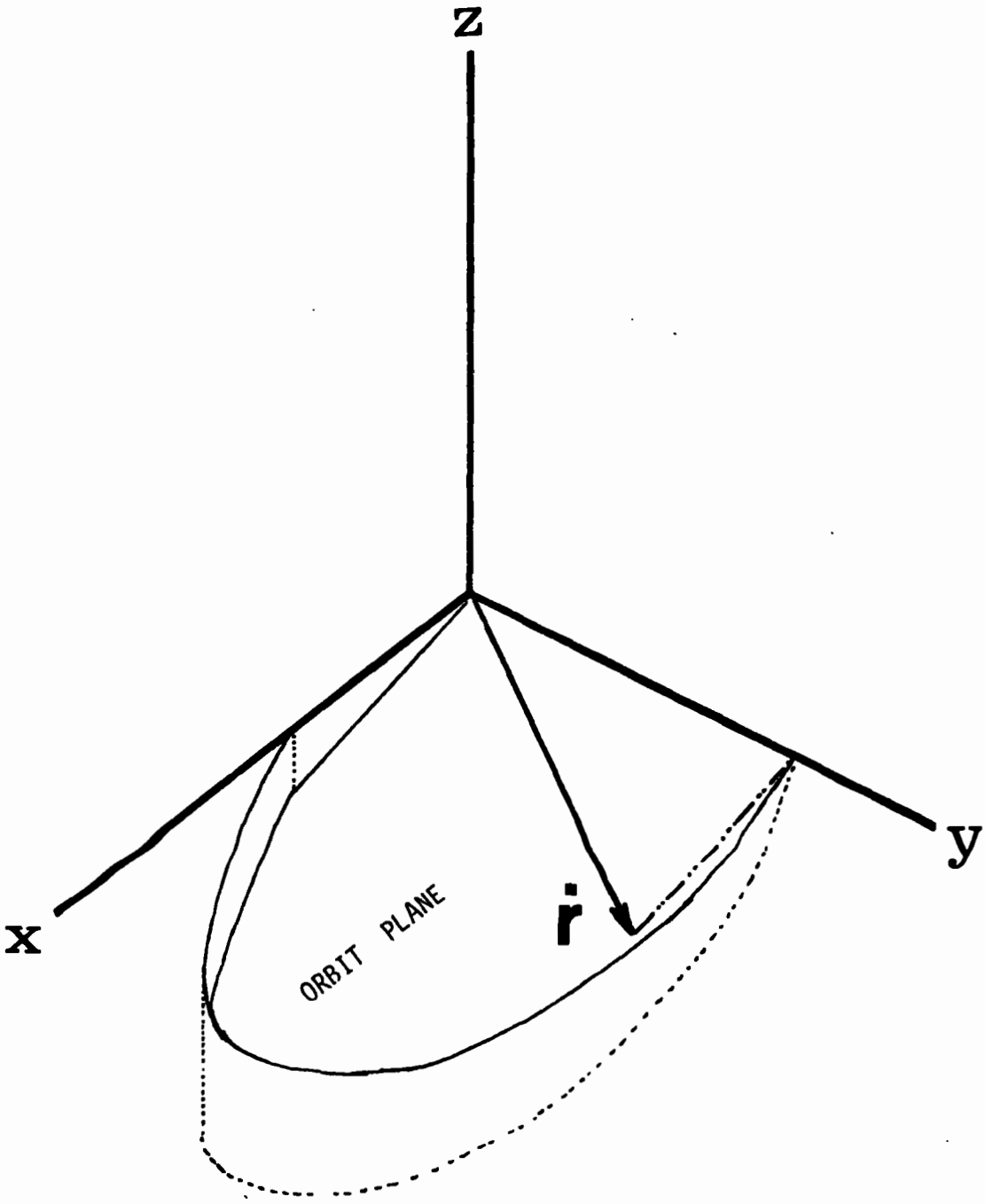


FIGURE 3.—*The "orbital" coordinate system.*

degree and order (up to 75) so that results from different models could be compared; second, to pick initial orbital conditions to generate a trajectory such that positions at which the gradients are computed would reflect as much as possible the effect of accurately observed data. Our practice was, for a given set of initial conditions, to run three gravitational models, of maximum degree and order 25, 70, and 75, for 24 time steps of 30 seconds each (i.e., a 12-minute time arc, covering a ground path of about 5,300 km). Initial conditions were chosen such that the satellite trajectory began at 300-km height and passed over selected areas of the Unite States and surroundings, or Europe and North Africa. Although the program had the ability to handle other perturbations, such as drag, radiation pressure, and luni-solar gravitation, these options were not employed, so subsequent positions of the

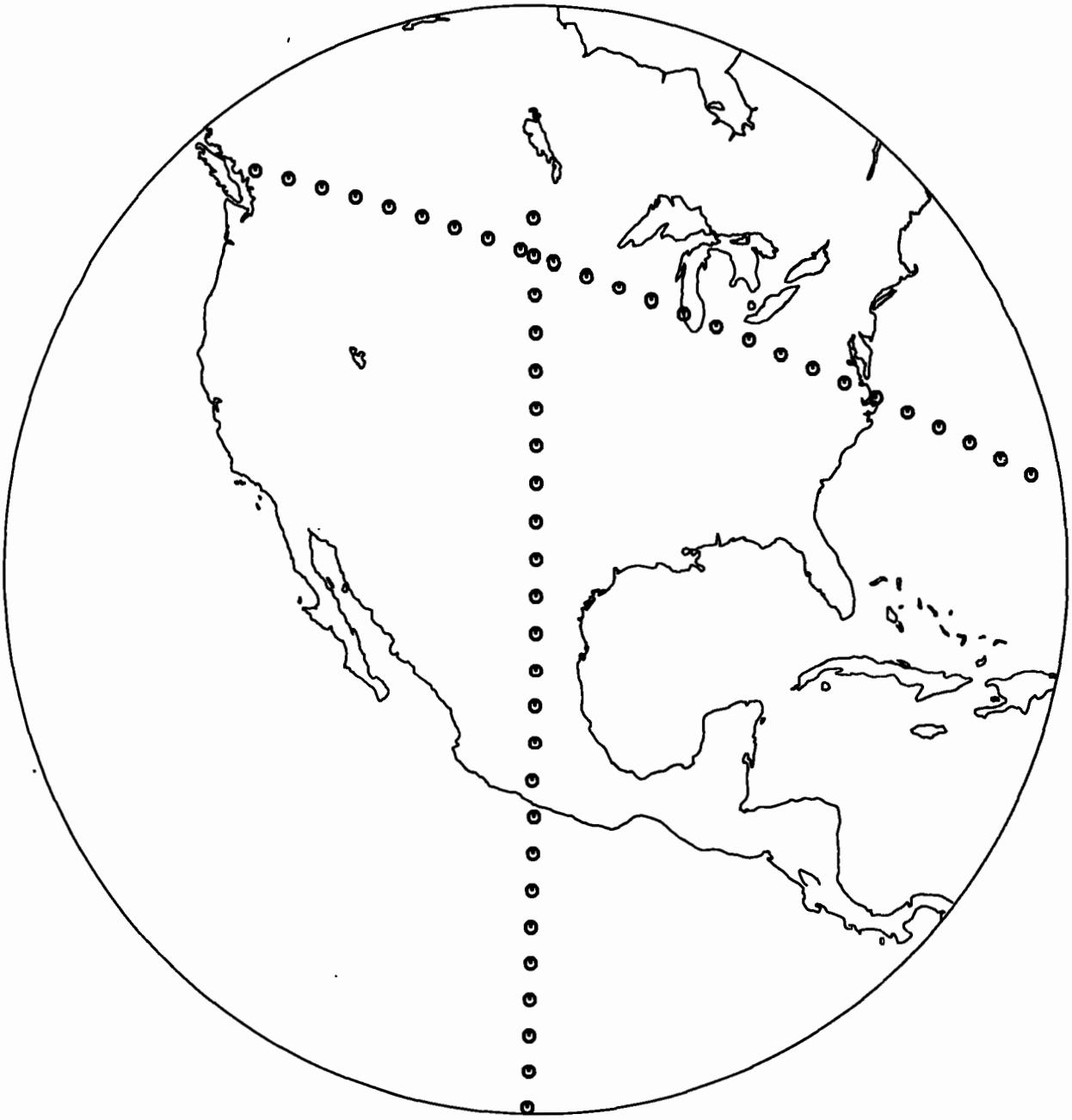

FIGURE 4.—*Satellite paths corresponding to tables 4 and 5.*

hypothetical arc were not completely realistic. Plots of satellite paths chosen and points at which the gravity gradient computations were made are shown in figures 4 and 5.

A sample computer output is displayed in figure 6. For each point at which the gravity gradient is computed, a grouping of five lines includes the time, and the position, velocity, and acceleration of the satellite in the particular coordinate system chosen (in this case the "gravity" coordinate system). In addition various orbital information is presented. The six gravity gradients are contained in the matrix at the end of the top three lines.

## 3. SIMPLE AVERAGING OF RESULTS

Tables 1 through 5 illustrate the results at 2.5-minute intervals obtained with the smaller data set. Differences of gravity gradient components of different models are listed. The components are all in the "gravity" system. Tables 1 through 4 compare results from three models, viz., maximum $l$ of 25,

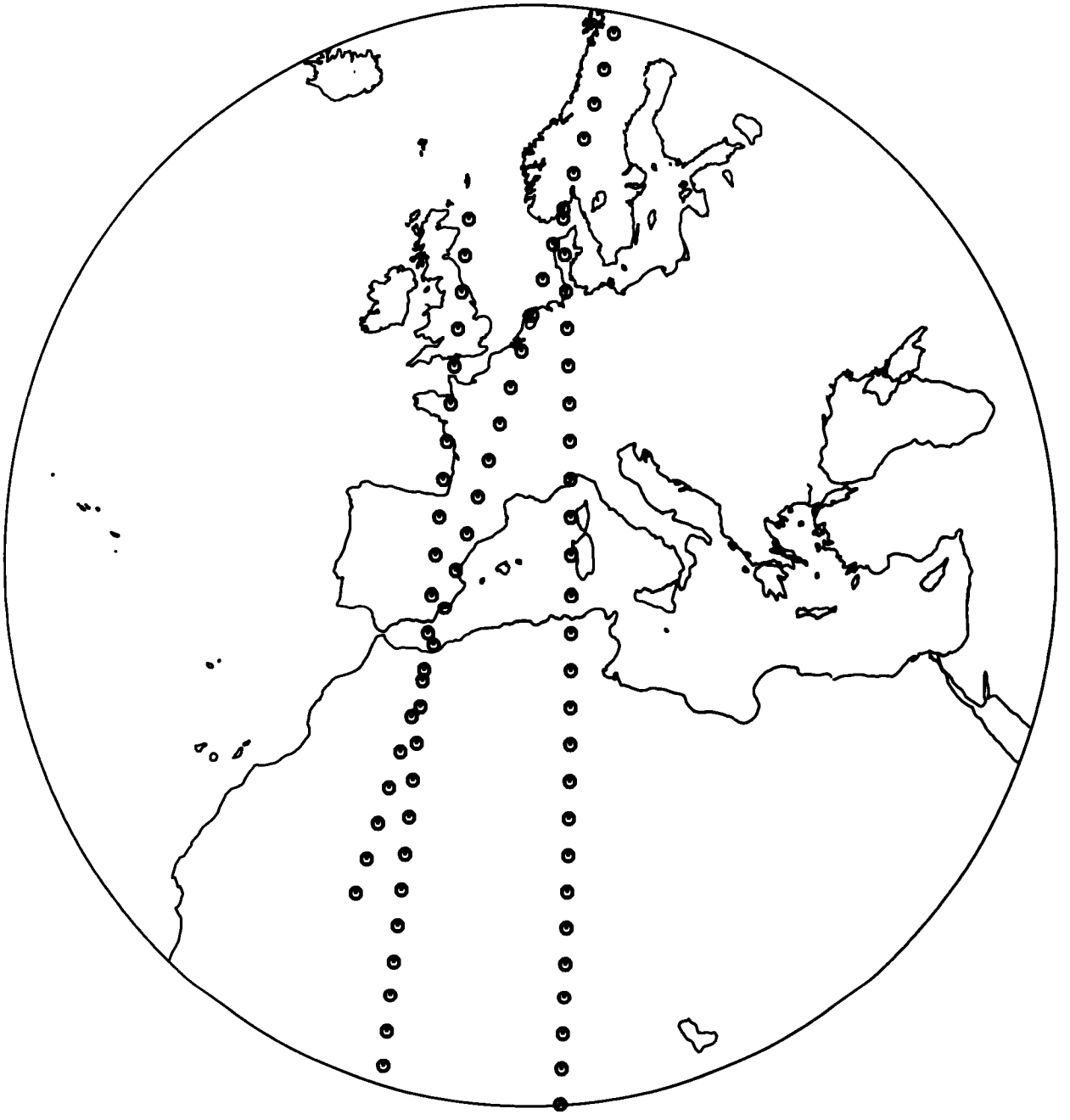

FIGURE 5.—*Satellite paths corresponding to tables 1, 2, and 3.*

```
1971 JAN.   1  1 39 30.0000  POS.     -955159.1     5412357.6     3749829.6 M        N(1,1)  -1352.2310  N(R,S)  GRAVITY CS  IN EOTVOS
            40952.06909722  VEL.     3092301.5    16175030.6   -22499015.9 M/HR     N(2,S)       .4985     -1354.7849
        ALT.=  282.0 KM     ACC.    16738624.5   -94850035.7   -65908958.2 M/HRSQ   N(3,S)       .1166       -1.6695      2707.0159
                ELEMENTS- OSC.  A=   6661668.6  E= .0017360050  I=  99.9915068  NODE= 273.1045968 A/P= 100.9660392  M=     .1221841
                    LAT.=      34.479   LONG.=     -24.657       GST=   8.3109927  TRUE=  44.1246423    EA=  44.0554352

1971 JAN.   1  1 40  0.0000  POS.     -928814.0     5543829.0     3560087.6 M        N(1,1)  -1352.3520  N(R,S)  GRAVITY CS  IN EOTVOS
            40952.06944444  VEL.     3229887.0    15374890.5   -23034444.1 M/HR     N(2,S)       .5084     -1355.0521
        ALT.=  281.6 KM     ACC.    16278435.7   -97163864.4   -62580407.5 M/HRSQ   N(3,S)       .0873       -1.7309      2707.4041
                ELEMENTS- OSC.  A=   6662286.4  E= .0017988768  I=  99.9911353  NODE= 273.1049187 A/P= 103.1778394  M=     .1215859
                    LAT.=      32.517   LONG.=     -25.279       GST=   8.3193489  TRUE=  43.9137453    EA=  43.8423062

1971 JAN.   1  1 40 30.0000  POS.     -901338.5     5668553.6     3366000.2 M        N(1,1)  -1352.5214  N(R,S)  GRAVITY CS  IN EOTVOS
            40952.06979167  VEL.     3363553.0    14555961.6   -23541806.8 M/HR     N(2,S)       .4810     -1355.3029
        ALT.=  281.3 KM     ACC.    15798107.1   -99358943.7   -59174178.9 M/HRSQ   N(3,S)       .0936       -1.6778      2707.8243
                ELEMENTS- OSC.  A=   6662885.2  E= .0018566555  I=  99.9905750  NODE= 273.1052098 A/P= 105.3547281  M=     .1210854
                    LAT.=      30.552   LONG.=     -25.881       GST=   8.3277050  TRUE=  43.7376716    EA=  43.6641753

1971 JAN.   1  1 41  0.0000  POS.     -872766.1     5786379.0     3167803.9 M        N(1,1)  -1352.6779  N(R,S)  GRAVITY CS  IN EOTVOS
            40952.07013889  VEL.     3493134.1    13719246.7   -24020475.8 M/HR     N(2,S)       .4744     -1355.4978
        ALT.=  281.0 KM     ACC.    15298184.8  -101432295.5   -55694533.5 M/HRSQ   N(3,S)       .1571       -1.6569      2708.1757
                ELEMENTS- OSC.  A=   6663462.8  E= .0019091583  I=  99.9902264  NODE= 273.1054719 A/P= 107.4972290  M=     .1206811
                    LAT.=      28.585   LONG.=     -26.464       GST=   8.3360612  TRUE=  43.5958897    EA=  43.5205122

1971 JAN.   1  1 41 30.0000  POS.     -843131.4     5897161.1     2965740.3 M        N(1,1)  -1352.8076  N(R,S)  GRAVITY CS  IN EOTVOS
            40952.07048611  VEL.     3618470.4    12865769.1   -24469857.4 M/HR     N(2,S)       .5139     -1355.7474
        ALT.=  280.7 KM     ACC.    14779399.6  -103381357.6   -52145715.9 M/HRSQ   N(3,S)       .2121       -1.6024      2708.5550
                ELEMENTS- OSC.  A=   6664016.2  E= .0019560893  I=  99.9897915  NODE= 273.1057059 A/P= 109.6040107  M=     .1203767
                    LAT.=      26.615   LONG.=     -27.130       GST=   8.3444173  TRUE=  43.4897233    EA=  43.4126447

1971 JAN.   1  1 42  0.0000  POS.     -812470.5     6000764.8     2760055.8 M        N(1,1)  -1352.9046  N(R,S)  GRAVITY CS  IN EOTVOS
            40952.07083333  VEL.     3739407.2    11996576.2   -24889390.9 M/HR     N(2,S)       .5664     -1355.9037
        ALT.=  280.4 KM     ACC.    14242465.1  -105203420.1   -48532017.7 M/HRSQ   N(3,S)       .2033       -1.5029      2708.8083
                ELEMENTS- OSC.  A=   6664541.8  E= .0019971663  I=  99.9893723  NODE= 273.1059127 A/P= 111.6684578  M=     .1201906
                    LAT.=      24.644   LONG.=     -27.581       GST=   8.3527735  TRUE=  43.4257798    EA=  43.3471764

1971 JAN.   1  1 42 30.0000  POS.     -780820.6     6097053.4     2551001.4 M        N(1,1)  -1352.9644  N(R,S)  GRAVITY CS  IN EOTVOS
            40952.07118056  VEL.     3855796.1    11112738.1   -25278556.7 M/HR     N(2,S)       .5694     -1356.0814
        ALT.=  280.2 KM     ACC.    13688030.2  -106896210.6   -44858142.7 M/HRSQ   N(3,S)       .1516       -1.4934      2709.0458
                ELEMENTS- OSC.  A=   6665038.0  E= .0020323529  I=  99.9889726  NODE= 273.1060927 A/P= 113.6900922  M=     .1201241
                    LAT.=      22.671   LONG.=     -28.119       GST=   8.3611296  TRUE=  43.4145293    EA=  43.3245735
```

FIGURE 6.—*Sample computer output for gravity gradient determination.*



506-579 O - 73 - 2

70, and 75, respectively. In addition, table 5 lists results involving also 60, 61, and 71. Table 6 condenses tables 1 through 5 by showing the maximum and r.m.s. difference over a particular path.

The same set of orbital computations were carried out with the larger set of data, and table 7 presents a summary of results corresponding to table 6. Although the r.m.s. values are now slightly higher, the increase is not significant.

These computations indicate that 0.01 EU is of threshold sensitivity, when considering the magnitudes of a range, $71 \leq l \leq 75$, of sums of harmonics, and that better than 0.02 EU is needed for the range 61 to 70. These figures tend to confirm the previous results of Forward and Kaula, and the general validity of Kaula's rule-of-thumb. They also imply the absence of marked deviations from this rule up to at least $l=75$.

## 4. HARMONIC ANALYSIS OF RESULTS

To make a more refined analysis, the simulated data were subjected to a harmonic analysis. By this means we were able to ascertain not only the fact that there were differences in the gravity gradients produced by the different geopotential models used, but also the structure of these differences. Two recently derived spectral estimators were used, the maximum entropy (MEM) and the maximum likelihood (MLM) (Lacoss 1971).

The data $\underline{x}(t)$ are given at $N$ times uniformly spaced by an interval $\Delta t$:

$$\underline{x}(t) = \mathrm{col}\,(x_1, x_2, \ldots, x_N).$$

Before the processing, the mean value $\langle x \rangle$ is subtracted from the data

$$\langle x \rangle = \frac{1}{N} \sum_{i=1}^{N} x_i$$

$$x_i' = x_i - \langle x \rangle.$$

The algorithms for both these spectral estimators begin by generating a sequence of linear error filters from the data.

The value of the error $v_{ib}$ at a point $i$ predicted by a *backward linear error filter* of length $b$ is

$$\begin{aligned} v_{ib} &= x_i' - \hat{x}_i' \\ &= \underline{\Gamma}_b^T \underline{\xi}(\underline{x}'; i, b), \end{aligned} \tag{1}$$

where $\hat{x}_i'$ = predicted value of $x_i'$,

$$\underline{\Gamma}_b = \mathrm{col}(1, \gamma_1, \gamma_2, \ldots, \gamma_b)$$

is the filter, and

$$\underline{\xi}(\underline{x}'; i, b) = \mathrm{col}(x_i', x_{i+1}', \ldots, x_{i+b}').$$

The *error* $v_{ib}$ is the departure of the data from the $x_i'$ predicted by the linear prediction filter which is obtained by setting the first component of $\underline{\Gamma}_b$ to zero and changing the signs of the $\gamma$'s.

A *foward* error filter involves the use of values preceding the one predicted:

$$v_{ib} = \underline{\Gamma}_b^T \underline{\eta}(\underline{x}'; i, b), \tag{2}$$

where

$$\underline{\eta}(\underline{x}'; i, b) = \mathrm{col}\,(x_i', x_{i-1}', \ldots, x_{i-b}')$$

A sequence of filters of increasing dimension, $\underline{\Gamma}_b$, $b=0, \ldots, M \leq N-1$, is computed by a method due to J. P. Burg (1967, 1970).

$$\underline{\Gamma}_0 = 1$$

$$\underline{\Gamma}_1 = \mathrm{col}\,(1, \gamma_{11})$$

$$\underline{\Gamma}_2 = \mathrm{col}\,(1, \gamma_{21}, \gamma_{22})$$

$$\cdots$$

$$\underline{\Gamma}_M = \mathrm{col}\,(1, \gamma_{M1}, \gamma_{M2}, \ldots, \gamma_{MM}).$$

Each filter is a solution of the discrete Wiener-Hopf equations (Yule-Walker equations—Wiener 1942) as modified for an error filter:

(a) Each filter is related to the previous one in the sequence by the Levinson recursion procedure (Levinson 1947).

(b) At each stage of the Levinson recursion, a single new coefficient $\gamma_{ii}$ is left undetermined. By requiring that the sum of the mean square prediction errors from the forward application and the backward application of the filter be minimized, a value of $\gamma_{ii}$ is obtained (J. P. Burg 1967, 1970).

Only the given data are used to generate the filters; no explicit extension of the data is assumed. The covariance $\phi_n$ of $\underline{x}'$ for a lag of $n\Delta t$ and the power $p_n$ (mean square) of the residual errors are computed from $\underline{\Gamma}_n, p_{n-1}; \phi_{n-1}, \ldots, \phi_0$ by formulas

ancillary to Levinson's method. Covariances are estimated indirectly by means of the directly estimated filter coefficients rather than by the usual procedure of assuming an extension of the data and then computing estimates of covariances and $\underline{\Gamma}_n$ and $p_n$ in turn from them.

One of the consequences of using the Wiener-Hopf equations to generate the filters is that the errors (from a forward or backward application of the filter) $\underline{v}_b = (v_{1b}, v_{2b}, \ldots, v_{Nb})$ have zero covariance for the lags $q\Delta t$, $q = 1, \ldots, b$. As $b$ increases $\underline{v}_b$ approaches the state of being white noise (the covariance function of white noise is the Krönecker delta function) and the final error filter $\underline{\Gamma}_{N-1}$ is referred to as a *whitening filter*.

If we define

$$\underline{E}_b = \mathrm{col}\,(1, \exp j\lambda, \exp 2j\lambda, \ldots, \exp bj\lambda),$$

where $j = \sqrt{-1}$, and

$$\lambda = 2\pi f \Delta t,$$

the discrete Fourier transform of $\underline{\Gamma}_b$ is

$$F_\gamma(f) = \underline{\Gamma}_b^T \underline{E}_b.$$

The discrete Fourier transform of $\underline{x}'$ and $\underline{v}_b$ are

$$F_{\underline{x}'}(f) = (\underline{x}')^T \underline{E}_n$$

$$F_{\underline{v}_b}(f) = (\underline{v}_b)^T \underline{E}_{n+b-1}.$$

The coefficients in the product of the two polynomials in $\exp j\lambda$, $F_{\underline{x}'}$ and $F_\gamma$, are given by eq (2). Therefore

$$F_{\underline{x}'}(f) F_\gamma(f) = F_{\underline{v}_b}(f).$$

Denote

$$P_b(f) = \| F_{\underline{x}'}(f) \|^2 / w$$

and

$$p_b = \| F_{\underline{v}_b}(f) \|^2,$$

where $P_b(f)$ is the power spectral *density* in the Nyquist band $0 \leq f \leq w$, $w = 1/2\Delta t$, and $p_b$ is the power in the residual errors (independent of frequency for white noise and *nearly* constant even when $b < n$).

Thus

$$P_b(f) = p_b / w \| F_\gamma(f) \|^2. \tag{3}$$

Burg (1967, 1970) has shown that eq (3), used with a Wiener-Hopf whitening filter $\underline{\Gamma}$, produces the spectrum maximizing the entropy

$$S = \int_0^w ln\, P(f) df$$

and which also is consistent with the covariance values $\phi_n, \phi_{n-1}, \ldots, \phi_0$. This property gives rise to the name of the method.

The filter coefficients depend on the values of the data points, so MEM is known as the *data-adaptive* spectral estimator. In practice it gives spectra with sharp peaks and is good for resolving nearly commensurable frequencies present in data.

The computation of the maximum likelihood estimator is more involved than that for MEM. All the filters $\Gamma_1, \Gamma_2, \ldots, \Gamma_b$ must be retained, which requires a considerable amount of computer memory or the use of tape or disc stroage. A matrix $Q_b$ is defined as

$$Q_b = \begin{bmatrix} 1/P_b & 0 & 0 & \ldots & 0 \\ 0 & 1/P_{b-1} & 0 & & 0 \\ 0 & 0 & 1/P_{b-2} & & 0 \\ & & & & \\ \vdots & & & & \vdots \\ 0 & 0 & 0 & \ldots & 1/P_1 \end{bmatrix}$$

and a matrix $F_b$ is constructed from *all* the filters generated

$$F_b = \begin{bmatrix} 1 & 0 & 0 & \ldots & 0 \\ \gamma_{b1} & 1 & 0 & & 0 \\ \gamma_{b2} & \gamma_{b-1,2} & 1 & & 0 \\ \vdots & & & & \vdots \\ \vdots & & & & \vdots \\ \gamma_{b,b-1} & \gamma_{b-1,b-2} & \ldots & \ldots & 1 \end{bmatrix}$$

Then $R_b^{-1}$, the inverse of the covariance matrix, is given by

$$R_b^{-1} = F_b Q_b F_b^T.$$

The MLM estimator is, then,

$$L_b = 1/(E_b^T R_b^{-1} E_b^*)$$

where the star indicates complex conjugate. The estimator $L_j$ is also data-adaptive, because it, too, depends on the filters $\Gamma_b$, $\Gamma_{b-1}$, etc. In general the function $L_b(\gamma)$ is smoother than $P_b(\gamma)$ and displays less pronounced peaks. A relationship between $P_b(\gamma)$ and $L_b(\gamma)$ has been derived by Burg (1972), who introduced $P_b(\gamma)$.

Once the filter coefficients are computed, values of the spectral estimate for $[N/2]$ points equally spaced in the frequency domain are computed, where

$$[N/2] = \begin{cases} N/2, & N \text{ even} \\ (N-1)/2, & N \text{ odd} \end{cases}$$

The sequence of frequencies used $\{f_q\}$ is defined by

$$f_q = \frac{q}{N} \cdot \frac{1}{2\Delta t}, \; q = 1, \ldots, N.$$

An array is used to store the resulting tabulation of spectral estimates. A "binary chop" technique is used to determine possible maxima. The array is searched for maxima by testing for the conditions

$$P_j(f_q) \geq P_j(f_{q-1})$$

$$P_j(f_q) \geq P_j(f_{q+1}).$$

For whichever interval the difference is smaller, say $(q, q+1)$, an interpolated value is found

$$f_{q+1/2} = \frac{1}{2}(f_q + f_{q+1}),$$

and $P_b(f_{q+1/2})$ is computed. If a peak is not detected $P_b(f_{q-1/2})$ is computed. Then the test is made on the sequence $P_b(f_{q-1})$, $P_b(f_{q-1/2})$, $P_b(f_q)$. If the test fails again, then it must be that $P_b(f_q) \geq P_b(f_{q+1/2})$ and $P_b(f_q) \geq P_b(f_{q-1/2})$, so that the new test interval is $[f_{q-1/2}, f_{q+1/2}]$. The interval is reduced until the spectral values are all within 1 percent of each other, or the interval has been reduced by a factor of $2^{10}$. By this purely numerical means, the maxima of $P_b(f)$ are found. It is not expedient to attempt to find these maxima through the derivative of $P_b$, or correspondingly, to find maxima of $L_b$. The roots of the derivatives could not be found analytically, but only by a numerical procedure such as Newton-Raphsen.

Detecting frequency shifts in the gravity gradient components due to different gravity fields is only part of the problem. It also is necessary to estimate the amplitude of each of the frequencies in the signal. Some numerical experiments proved that the use of the amplitude of the *MLM* (maxima of $L_b$) was not a satisfactory way to estimate signal component amplitude. A more rigorous and reliable amplitude estimate would have been to perform a quadrature of the spectrum in the vicinity of the peaks. Since most peaks were well separated, we chose to use a simple procedure—performing a quadrature on the data. We computed by the trapezoidal formula (Abramowitz and Stegun 1964)

$$\hat{c}(\mu) = \frac{1}{\pi} \int_0^{2\pi} x(\theta) \cos \mu\theta d\theta$$

$$\hat{s}(\mu) = \frac{1}{\pi} \int_0^{2\pi} x(\theta) \sin \mu\theta d\theta$$

$$\theta = 2\pi \frac{t - t_0}{t_N - t_o}, \; t_o \leq t \leq t_N.$$

If the signal is of the form

$$x(\theta) = c \cos \mu\theta + s \sin \mu\theta,$$

we will have

$$\hat{c}(\mu) = c\left[1 + \frac{\sin 4\pi\mu}{4\pi\mu} - \frac{s}{4\pi\mu}(\cos 4\pi\mu - 1)\right]$$

$$\hat{s}(\mu) = s\left[1 - \frac{\sin 4\pi\mu}{4\pi\mu} - \frac{c}{4\pi\mu}(\cos 4\pi\mu - 1)\right].$$

The amplitude of the signal is

$$A(\mu) = (c^2 + s^2)^{1/2}.$$

We can solve for $A(\mu)$ in terms of $\hat{c}(\mu)$ and $\hat{s}(\mu)$ by successive approximations

$$A^2 = \hat{c}^2 + \hat{s}^2 + \frac{\hat{s}^2 - \hat{c}^2}{2\pi\mu} \sin 4\pi\mu + \frac{\hat{c}\hat{s}}{\pi\mu}(\cos 4\pi\mu - 1) + 0(1/\mu^2)$$

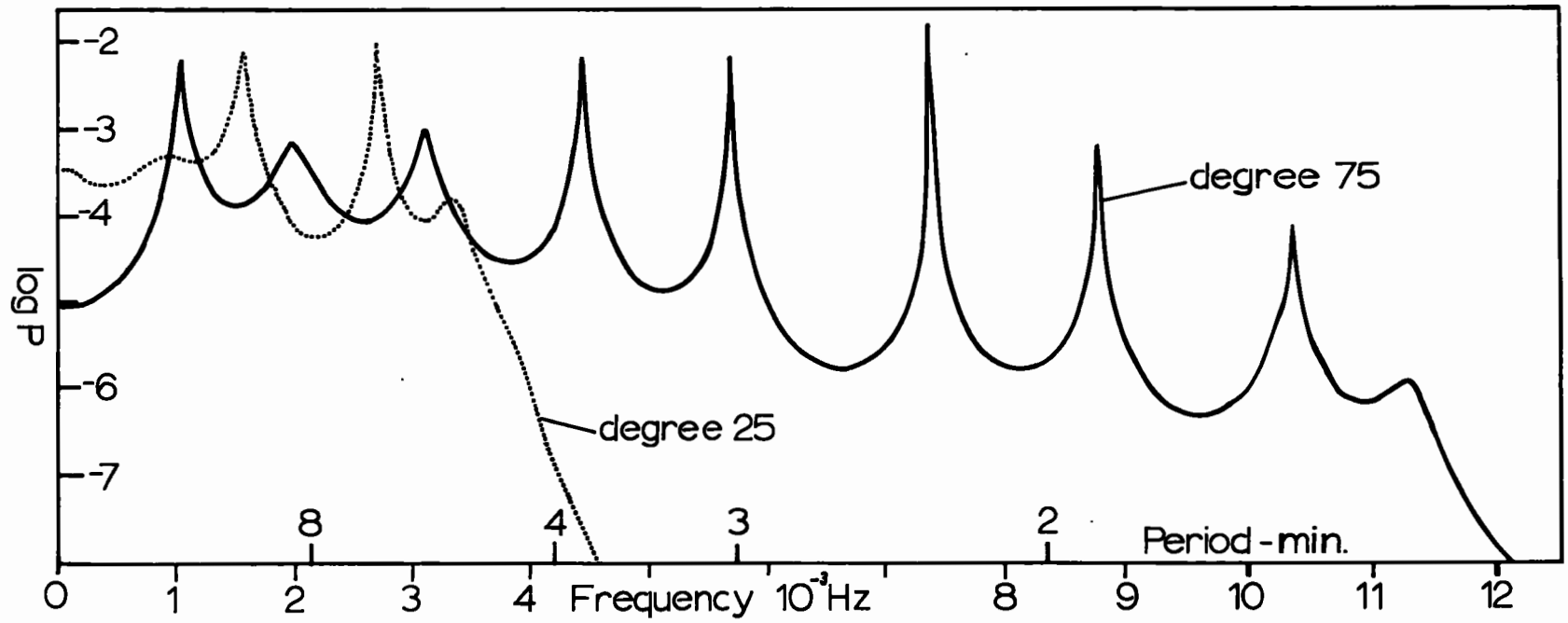


FIGURE 7.—*Graph of spectra tabulated in table 8.*

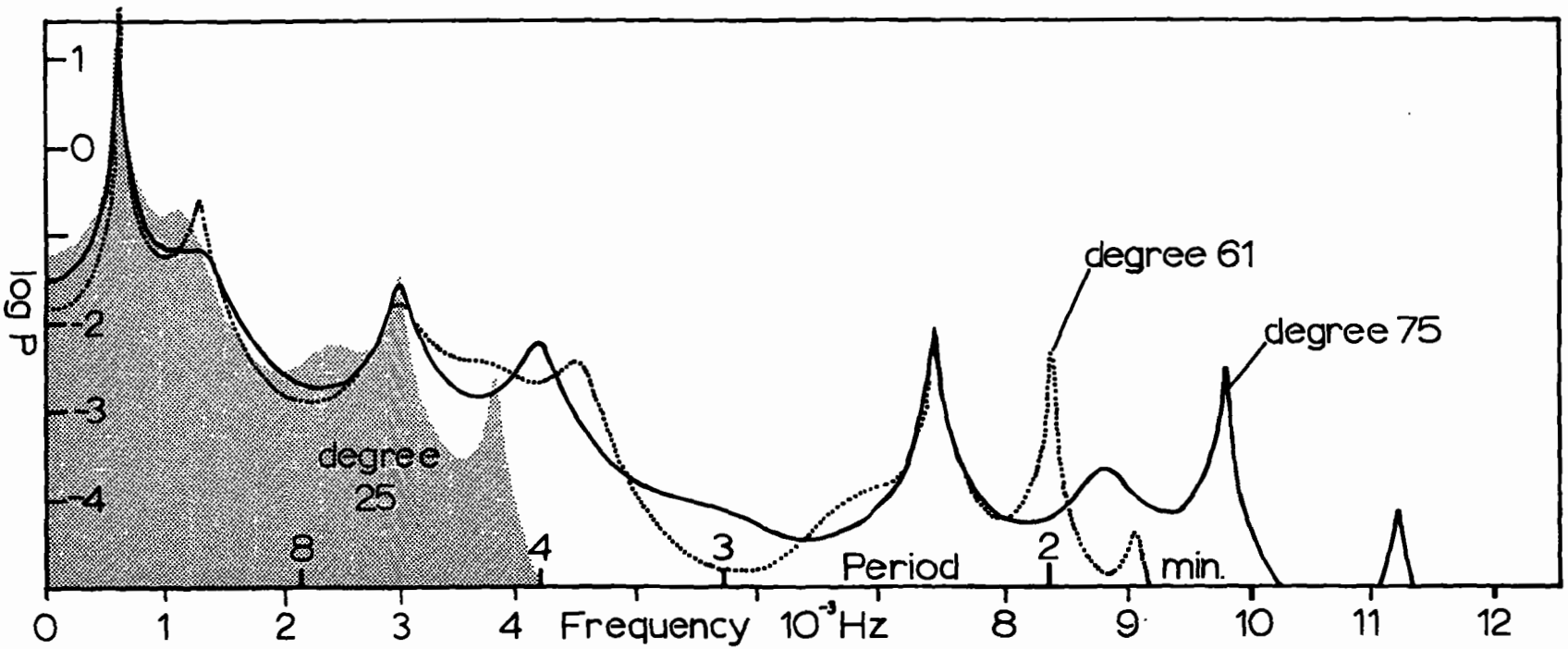


FIGURE 8.—*Graph of spectra tabulated in table 9.*

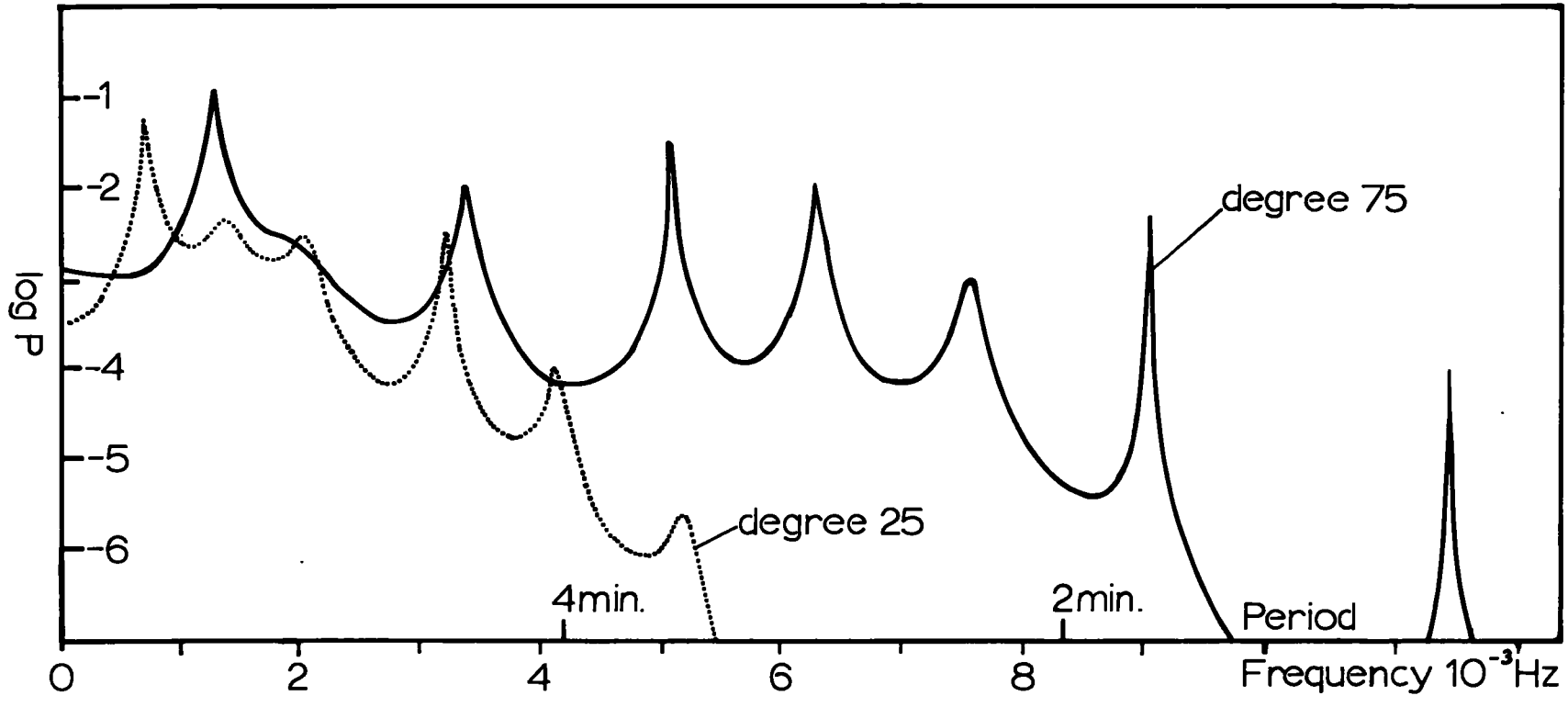


FIGURE 9.—*Graph of spectra tabulated on left side of table 10.*

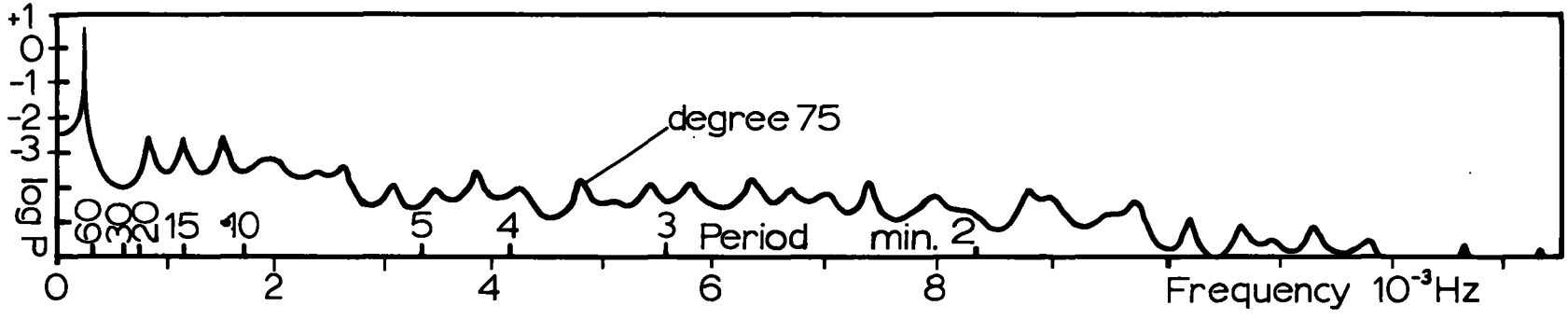


FIGURE 10.—*Graph of spectra tabulated on right side of table 10.*

All the signal components need not be mutually orthogonal over the data span; but no correction was computed for this.

The gravity gradients could have been computed by analytic means, using an extension of techniques developed by Douglas and Wagner (1968) to estimate the amplitudes of resonance perturbations for satellites. The quantity of algebraic manipulation and programming required does not make this method attractive, nor does the existence of 5,776 spherical harmonic coefficients of degree less than or equal to 75, each of which contributes one or more components to the gravity gradients. With gravity gradients there is no dynamical effect such as resonance that serves to amplify the effects of certain harmonics, so all are thoroughly mixed in the signal.

Another approach would have been to do a complete simulation of an adjustment using generated gradiometer data for a complete coverage of the entire earth. Again, the amount of computation would have been prohibitive. The question of parameterizations for the gravitational field would become paramount, since the gradiometry can give useful information about short wavelengths in the gravity field, but is unlikely to successfully resolve the 5,776 spherical harmonic coefficients.

The number of sinusoids with amplitudes greater than 0.01 EU, and the amplitudes themselves, give us some idea of the amount of information in the signal. One orbit was computed for a full revolution, instead of for just a short arc, to obtain some idea of how much more information comes from more extensive coverage. Tables 10 and 11 give a partial tabulation of these results.

The results in tables 8 through 11 and figures 7 through 10 confirm, in general, the initial evaluation of the results. The harmonic analysis does reveal the existence of a large number of components in the gravity gradient that are well separated in frequency, mostly with amplitudes a little larger than 0.03 EU. This more refined analysis indicates that an instrument sensitivity of 0.01 EU will not be just at the threshold of yielding useful information on the short wave components of the geopotential, but well beyond it.

For the purposes of this study we ignored the fact that the gravity gradient is a signal with five independent, but correlated channels. To simulate the data recording process, we analyzed the gravity gradient components in the "gravity" coordinate system, which is still somewhat different from the signal anticipated by Glaser (1971). Our results will be more adaptable, however, to variations in the instrumentation configuration.

These spectral analysis methods should be useful for examining actual data when it becomes available. Comparisons with simulated data in number of peaks present and their amplitudes could be made. This would allow one to assess the quality of the data before attempting to use it in any kind of solution for gravity or geopotential.

## ACKNOWLEDGMENTS

This study was partially supported by NASA Langley Research Center work order L-67767. Allen Pope of the Geodetic Research and Development Laboratory supplied much of the theory for the harmonic analysis.

## REFERENCES

Abramowitz, Milton, and Stegun, Irene A., *Handbook of Mathematical Functions*, U.S. Government Printing Office, Washington, D.C., 1964, p. 885.

Aeronautical Chart and Information Center, "1°×1° Mean Free-Air Gravity Anomalies," *ACIC Reference Publ.* No. 29, Defense Mapping Agency—Aerospace Center, St. Louis, Mo., 1971, 324 pp.

Burg, J. P., "Maximum Entropy Spectral Analysis," paper presented at 37th Annual International Meeting, Society of Exploration Geophysicists, Oklahoma City, Okla., Oct. 31, 1967, 5 pp.

Burg, J. P., "New Concepts in Power Spectra Estimation," paper presented at 40th Annual International Meeting, Society of Exploration Geophysicists, New Orleans, La., Nov. 11, 1970; abstract in *Geophysics*, Vol. 35, No. 6, 1970, p. 1158.

Burg, J. P., "The Relationship Between Maximum Entropy Spectra and Maximum Likelihood Spectra," *Geophysics*, Vol. 37, No. 2, 1972, pp. 375–376.

Douglas, B. C., and Wagner, C. A., "A Perturbation Analysis of Existing Resonant Satellites," *Goddard Space Flight Center Report* No. X-643-68-338, Greenbelt, Md., 1968, 61 pp.

Forward, R., "Geodesy with Orbiting Gravity Gradiometers," in *The Use of Artificial Satellites for Geodesy, American Geophysical Union Monograph* No. 15, Washington, D.C., 1972, pp. 239–243.

Glaser, R., "The Relation of Spherical Harmonics to Gravity Gradients," Abstract, E⊕S Trans-

actions of American Geophysical Union, Vol. 52, No. 11, 1971, p. 818.

Gulick, L., "A Comparison of Methods for Computing Gravitational Potential Derivatives," *ESSA Technical Report* C & GS 40, National Ocean Survey, National Oceanic and Atmospheric Administration, U.S. Department of Commerce, Rockville, Md., 1970, 32 pp.

Hotine, M., *Mathematical Geodesy, ESSA Monograph* No. 2, U.S. Government Printing Office, Washington, D.C., 1969, p. 86.

Kaula, W., ed., "The Terrestrial Environment, Solid-Earth and Ocean Physics," *Report of a Study at Williamstown, Mass. to NASA*, Massachusetts Institute of Technology, Cambridge, Mass., 1969, 147 pp.

Kaula, W., "Implications of New Techniques in Satellite Geodesy," paper presented at XV General Assembly, International Union of Geodesy and Geophysics, Moscow, USSR, 1971, 2 pp.

Lacoss, R. T., "Data Adaptive Spectral Analysis Methods," *Geophysics*, Vol. 36, No. 4, 1971, pp. 661–675.

Levinson, N., "An Heuristic Exposition of Weiner's Mathematical Theory of Prediction and Filtering," *Journal of Mathematical Physics*, Vol. 26, 1947, pp. 110–119.

Meissl, P., "A Study of Covariance Functions Related to the Earth's Disturbing Potential," *Ohio State University Dept. of Geodetic Science Report* No. 151, Columbus, Ohio, 1971, 88 pp.

Wiener, N., *Extrapolation, Interpolation, and Smoothing of Stationary Time Series with Engineering Applications*, Massachusetts Institute of Technology Press, Cambridge, Mass., 1942, 123 pp.

Witte, B., "Computational Procedures for the Determination of a Simple Layer Model of the Geopotential from Doppler Observations," *NOAA Technical Report* NOS 42, National Ocean Survey, National Oceanic and Atmospheric Administration, Rockville, Md., 1971, 63 pp.

TABLE 1.—*Gravity gradient component differences for satellite ground track starting at $\phi = 70°$ N, $\lambda = 20°$ E, and initial azimuth = 210°*

| $\lvert l_2 - l_1 \rvert$ | $\Delta t$ (min.) | $\Delta N_{qs}$ | | | | | |
|---|---|---|---|---|---|---|---|
| | | (1,1) | (2,1) | (2,2) | (3,1) | (3,2) | (3,3) |
| \| 70–25 \| | 2½ | 0.0983 | 0.0491 | 0.0372 | 0.0491 | 0.0507 | 0.1355 |
| | 5 | .0406 | .0093 | .0507 | .1976 | .0211 | .0101 |
| | 7½ | .0200 | .0414 | .0050 | .0356 | .0361 | .0250 |
| | 10 | .0891 | .0924 | .2074 | .1254 | .0780 | .2966 |
| | 12½ | .0024 | .0057 | .0140 | .0090 | .1254 | .0116 |
| \| 75–70 \| | 2½ | 0.0254 | 0.0001 | 0.0182 | 0.0074 | 0.0098 | 0.0436 |
| | 5 | .0080 | .0006 | .0190 | .0033 | .0036 | .0270 |
| | 7½ | .0061 | .0049 | .0137 | .0135 | .0037 | .0197 |
| | 10 | .0007 | .0059 | .0052 | .0171 | .0127 | .0045 |
| | 12½ | .0174 | .0056 | .0218 | .0023 | .0043 | .0392 |

TABLE 2.—*Gravity gradient component differences for satellite ground track starting at $\phi = 60°$ N, $\lambda = 10°$ E, and initial azimuth = 180°*

| $\lvert l_2 - l_1 \rvert$ | $\Delta t$ (min.) | $\Delta N_{qs}$ | | | | | |
|---|---|---|---|---|---|---|---|
| | | (1,1) | (2,1) | (2,2) | (3,1) | (3,2) | (3,3) |
| \| 70–25 \| | 2½ | 0.1506 | 0.0598 | 0.1376 | 0.0289 | 0.0150 | 0.2882 |
| | 5 | .0057 | .0324 | .0529 | .0380 | .0764 | .0472 |
| | 7½ | .0938 | .0123 | .1357 | .0151 | .1262 | .2295 |
| | 10 | .0784 | .0546 | .0850 | .0525 | .0905 | .1634 |
| | 12½ | .0636 | .0320 | .0639 | .0159 | .0219 | .0003 |
| \| 75–70 \| | 2½ | 0.0068 | 0.0019 | 0.0035 | 0.0028 | 0.0191 | 0.0033 |
| | 5 | .0005 | .0044 | .0078 | .0110 | .0108 | .0084 |
| | 7½ | .0215 | .0007 | .0064 | .0075 | .0270 | .0279 |
| | 10 | .0072 | .0003 | .0035 | .0133 | .0103 | .0106 |
| | 12½ | .0072 | .0051 | .0046 | .0194 | .0110 | .0118 |

TABLE 3.—*Gravity gradient component differences for satellite ground track starting at $\phi = 60°$ N, $\lambda = 0°$ E, and initial azimuth = 180°*

| $\lvert l_2 - l_1 \rvert$ | $\Delta t$ (min.) | $\Delta N_{qs}$ | | | | | |
|---|---|---|---|---|---|---|---|
| | | (1,1) | (2,1) | (2,2) | (3,1) | (3,2) | (3,3) |
| \| 70–25 \| | 2½ | 0.0694 | 0.0557 | 0.0240 | 0.1017 | 0.0195 | 0.0455 |
| | 5 | .0751 | .0372 | .0631 | .0806 | .0919 | .0120 |
| | 7½ | .0478 | .0171 | .0285 | .1199 | .1894 | .0763 |
| | 10 | .0390 | .0229 | .0514 | .0155 | .0850 | .0124 |
| | 12½ | .0547 | .0146 | .1025 | .0626 | .0337 | .1573 |
| \| 75–70 \| | 2½ | 0.0067 | 0.0061 | 0.0110 | 0.0126 | 0.0041 | 0.0177 |
| | 5 | .0044 | .0084 | .0141 | .0081 | .0089 | .0184 |
| | 7½ | .0056 | .0040 | .0124 | .0006 | .0009 | .0179 |
| | 10 | .0033 | .0066 | .0078 | .0162 | .0075 | .0111 |
| | 12½ | .0074 | .0020 | .0065 | .0034 | .0003 | .0010 |

TABLE 4.—*Gravity gradient component differences for satellite ground track starting at $\phi=50°$ N° 100° W, and initial azimuth=180°*

| $\lvert l_2-l_1 \rvert$ | $\Delta t$ (min.) | $\Delta N_{\varphi\varphi}$ | | | | | |
|---|---|---|---|---|---|---|---|
| | | (1,1) | (2,1) | (2,2) | (3,1) | (3,2) | (3,3) |
| \|70–25\| | 2½ | 0.0355 | 0.0054 | 0.0017 | 0.0700 | 0.0012 | 0.0372 |
| | 5 | .0016 | .0600 | .0072 | .0036 | .0369 | .0056 |
| | 7½ | .0947 | .1224 | .1418 | .0827 | .0456 | .2365 |
| | 10 | .0342 | .0253 | .0487 | .0027 | .0119 | .0829 |
| | 12½ | .0232 | .0262 | .0202 | .0367 | .0209 | .0030 |
| \|75–70\| | 2½ | 0.0103 | 0.0028 | 0.0155 | 0.0004 | 0.0002 | 0.0259 |
| | 5 | .0123 | .0056 | .0029 | .0011 | .0189 | .0094 |
| | 7½ | .0044 | .0007 | .0063 | .0179 | .0101 | .0106 |
| | 10 | .0006 | .0072 | .0010 | .0115 | .0084 | .0004 |
| | 12½ | .0021 | .0051 | .0028 | .0084 | .0031 | .0049 |

TABLE 5.—*Gravity gradient component differences for satellite ground track starting at $\phi=50°$ N, $\lambda=125°$ W, and initial azimuth=90°.*

| $\lvert l_2-l_1 \rvert$ | $\Delta t$ (min.) | $\Delta N_{\varphi\varphi}$ | | | | | |
|---|---|---|---|---|---|---|---|
| | | (1,1) | (2,1) | (2,2) | (3,1) | (3,2) | (3,3) |
| \|60–25\| | 2½ | 0.0420 | 0.0089 | 0.0270 | 0.0343 | 0.0239 | 0.0149 |
| | 5 | .0073 | .0123 | .0820 | .0382 | .0565 | .0747 |
| | 7½ | .0090 | .0098 | .0202 | .0356 | .0246 | .0112 |
| | 10 | .0006 | .0219 | .0219 | .0388 | .1169 | .0225 |
| | 12½ | .0187 | .0178 | .0495 | .0002 | .0030 | .0681 |
| \|61–60\| | 2½ | .0065 | .0028 | .0045 | .0018 | .0061 | .0108 |
| | 5 | .0037 | .0023 | .0114 | .0184 | .0083 | .0150 |
| | 7½ | .0016 | .0051 | .0090 | .0025 | .0119 | .0074 |
| | 10 | .0045 | .0029 | .0035 | .0020 | .0138 | .0011 |
| | 12½ | .0028 | .0178 | .0047 | .0074 | .0138 | .0019 |
| \|70–61\| | 2½ | .0053 | .0036 | .0015 | .0232 | .0031 | .0068 |
| | 5 | .0042 | .0048 | .0183 | .0232 | .0654 | .0226 |
| | 7½ | .0080 | .0047 | .0001 | .0136 | .0055 | .0081 |
| | 10 | .0022 | .0031 | .0159 | .0078 | .0069 | .0181 |
| | 12½ | .0189 | .0025 | .0093 | .0181 | .0273 | .0096 |
| \|71–70\| | 2½ | .0017 | .0017 | .0038 | .0065 | .0038 | .0056 |
| | 5 | .0033 | .0007 | .0043 | .0034 | .0064 | .0077 |
| | 7½ | .0009 | .0011 | .0043 | .0029 | .0047 | .0032 |
| | 10 | .0038 | .0067 | .0042 | .0005 | .0004 | .0080 |
| | 12½ | .0029 | .0016 | .0025 | .0058 | .0060 | .0054 |
| \|75–71\| | 2½ | .0029 | .0045 | .0070 | .0049 | .0049 | .0040 |
| | 5 | .0131 | .0053 | .0030 | .0032 | .0006 | .0161 |
| | 7½ | .0000 | .0028 | .0061 | .0079 | .0064 | .0060 |
| | 10 | .0118 | .0038 | .0022 | .0043 | .0026 | .0140 |
| | 12½ | .0163 | .0053 | .0001 | .0168 | .0005 | .0164 |

TABLE 6.—*Summary of maximum and r.m.s. differences of gravity gradients of various models for smaller data set*

| $\phi$ | $\lambda$ | az. | \|70–25\| | | \|75–70\| | |
|---|---|---|---|---|---|---|
| | | | max. | r.m.s. | max. | r.m.s. |
| 70 | 20 | 210 | 0.02966 | 0.0949 | 0.0436 | 0.0163 |
| 60 | 10 | 180 | .2882 | .1005 | .0279 | .0117 |
| 60 | 0 | 180 | .1894 | .0736 | .0184 | .0094 |
| 50 | −100 | 180 | .2365 | .0674 | .0259 | .0094 |
| 50 | −125 | 90 | 0.1169 | 0.0402 | \|60–25\| | |
| | | | .0184 | .0085 | \|61–60\| | |
| | | | .0232 | .0126 | \|70–61\| | |
| | | | .0080 | .0042 | \|71–70\| | |
| | | | .0164 | .0082 | \|75–71\| | |

TABLE 7.—*Summary of maximum and r.m.s. differences of gravity gradients of various models for larger data set*

| $\phi$ | $\lambda$ | az. | \|70–25\| | | \|75–70\| | |
|---|---|---|---|---|---|---|
| | | | max. | r.m.s. | max. | r.m.s. |
| 70 | 20 | 210 | 0.3675 | 0.1149 | 0.0418 | 0.0167 |
| 60 | 10 | 180 | .2901 | .1067 | .0365 | .0153 |
| 60 | 0 | 180 | .1939 | .0769 | .0218 | .0083 |
| 50 | −100 | 180 | .3269 | .0891 | .0229 | .0088 |
| 50 | −125 | 90 | 0.1160 | 0.0481 | \|60–25\| | |
| | | | .0133 | .0058 | \|61–60\| | |
| | | | .0462 | .0182 | \|70–61\| | |
| | | | .0182 | .0058 | \|71–70\| | |
| | | | .0217 | .0102 | \|75–71\| | |

TABLE 8.—*Amplitudes of harmonic components of gravity gradients* $N_{21}$ *for fields of degree and order 25, 70, 75; the trajectory is the one described in the caption of table 2*

| Period (minutes) | MEM Peak $P_{20}$ (EU)$^2$ | Amplitude (EU) | Period (minutes) | MEM Peak $P_{20}$ (EU)$^2$ | Amplitude (EU) |
|---|---|---|---|---|---|
| Degree and order 25 | | | | | |
| 14.6 | $5.8\times10^{-4}$ | 0.04 | 1.9 | $5.3\times10^{-3}$ | .017 |
| 8.7 | $7.4\times10^{-3}$ | .04 | 1.7 | $4.4\times10^{-3}$ | .014 |
| 5.1 | $9.2\times10^{-3}$ | .05 | 1.4 | $3.5\times10^{-6}$ | .0035 |
| 4.1 | $1.8\times10^{-4}$ | .02 | | | |
| 1.9 | $1.2\times10^{-10}$ | .0018 | Degree and order 75 | | |
| 1.6 | $3.3\times10^{-11}$ | .0018 | 13.5 | $6.5\times10^{-3}$ | 0.034 |
| 1.3 | $8.2\times10^{-11}$ | .0017 | 7.0 | $8.0\times10^{-4}$ | .018 |
| | | | 4.5 | $1.0\times10^{-3}$ | .023 |
| Degree and order 70 | | | 3.1 | $6.8\times10^{-3}$ | .032 |
| 13.2 | $7.2\times10^{-3}$ | 0.03 | 2.4 | $6.9\times10^{-3}$ | .024 |
| 6.8 | $5.4\times10^{-4}$ | .017 | 1.86 | $1.2\times10^{-2}$ | .018 |
| 4.2 | $5.1\times10^{-4}$ | .016 | 1.57 | $6.6\times10^{-4}$ | .012 |
| 3.1 | $6.6\times10^{-3}$ | .033 | 1.33 | $6.3\times10^{-5}$ | .006 |
| 2.4 | $3.5\times10^{-3}$ | .022 | 1.22 | $1.3\times10^{-6}$ | .005 |

TABLE 9.—*Amplitudes of harmonic components of gravity gradient* $N_{22}$ *for fields of degree and order 25, 60, 61, 70, 71, 75; trajectory is the one described in the caption of table 5*

| Period (minutes) | MEM Peak $P_{20}$ (EU)$^2$ | Amplitude (EU) |
|---|---|---|
| Degree and order 25 | | |
| 24.2 | 11.3 | 1.41 |
| 12.7 | .27 | 1.23 |
| 5.8 | .0067 | 0.41 |
| 4.7 | .033 | 0.20 |
| 3.6 | .0023 | 0.15 |
| 1.57 | $1.2\times10^{-9}$ | 0.12 |
| 1.42 | $2.6\times10^{-10}$ | 0.08 |
| 1.20 | $1.2\times10^{-8}$ | 0.09 |
| Degree and order 60 | | |
| 23.5 | 14.1 | 1.43 |
| 11.3 | .15 | .97 |
| 4.8 | .065 | .13 |
| 3.4 | .016 | .15 |
| 2.9 | .0012 | .24 |
| 2.0 | .0075 | .18 |
| 1.78 | .028 | .15 |
| 1.69 | .018 | .13 |
| 1.06 | $2.5\times10^{-10}$ | .08 |
| Degree and order 61 | | |
| 23.6 | 36.8 | 1.43 |
| 11.2 | .27 | .95 |
| 4.7 | .022 | .20 |
| 3.1 | .0043 | .32 |
| 1.86 | .0056 | .05 |
| 1.66 | .0050 | .11 |
| 1.52 | $3.9\times10^{-5}$ | .13 |
| Degree and order 70 | | |
| 23.2 | 12.75 | 1.44 |
| 4.6 | .040 | .23 |
| 3.3 | .0056 | .27 |
| 2.3 | $9.8\times10^{-5}$ | .09 |
| 1.82 | .0025 | .11 |
| 1.43 | .0016 | .07 |
| 1.34 | $5.8\times10^{-5}$ | .12 |
| Degree and order 71 | | |
| 23.0 | 11.7 | 1.44 |
| 4.6 | .035 | .26 |
| 3.2 | .0054 | .30 |
| 2.3 | $1.4\times10^{-4}$ | .11 |
| 1.84 | .0035 | .09 |
| 1.65 | $5.6\times10^{-4}$ | .10 |
| 1.39 | .0088 | .12 |
| 1.26 | $4.5\times10^{-6}$ | .09 |
| Degree and order 75 | | |
| 23.4 | 18.6 | 1.43 |
| 11.4 | .095 | .98 |
| 4.6 | .037 | .23 |
| 3.3 | .0070 | .25 |
| 1.86 | .012 | .06 |
| 1.56 | $2.4\times10^{-4}$ | .12 |
| 1.40 | .0033 | .10 |
| 1.22 | $8.2\times10^{-5}$ | .11 |

TABLE 10.—*Spectral analysis of simulated gravity gradients for a full revolution. These are results for the $N_{31}$ component. Comparison is made with 30-minute data spans using 25, 25, fields and 75, 75 fields. The trajectory is the one described in the caption of table 1. The complete revolution is a forward extension of the short arc of table 1.*

| Period (minutes) | MEM Peak $P_{20}$ (EU)$^2$ | Amplitude (EU) | Period (minutes) | MEM Peak $P_{100}$ (EU)$^2$ | Amplitude (EU) |
|---|---|---|---|---|---|
| Degree and order 25 | | | Degree and order 75 one complete revolution | | |
| 20.8 | 0.061 | 0.13 | 85.1 | 4.0 | 0.66 |
| 10.3 | .006 | .13 | 21.1 | .0036 | .11 |
| 7.0 | .004 | .07 | 15.0 | .0033 | .04 |
| 4.4 | .004 | .015 | 11.3 | .0032 | .07 |
| 3.4 | $1.0\times10^{-4}$ | .009 | 8.5 | .0009 | .018 |
| 2.7 | $2.7\times10^{-6}$ | .007 | 7.0 | .0004 | .026 |
| 1.87 | $1.5\times10^{-9}$ | .005 | 6.4 | .0005 | .026 |
| 1.36 | $1.0\times10^{-9}$ | .006 | 5.4 | .0001 | .019 |
| 1.15 | $4.0\times10^{-10}$ | .005 | 4.8 | .0001 | .014 |
| | | | 4.4 | .0004 | .013 |
| Degree and order 70 | | | 3.9 | .0001 | .015 |
| 11.2 | 0.070 | 0.19 | 3.5 | .0002 | .015 |
| 4.0 | .007 | .07 | 3.3 | $5.0\times10^{-5}$ | .012 |
| 2.7 | .032 | .07 | 3.1 | .0002 | .015 |
| 2.3 | .011 | .05 | 2.9 | .0002 | .012 |
| 1.9 | .004 | .036 | 2.6 | .0002 | .021 |
| 1.57 | .0005 | .007 | 2.5 | .0001 | .011 |
| 1.36 | .0001 | .004 | 2.4 | $7.9\times10^{-5}$ | .008 |
| | | | 2.3 | .0002 | .012 |
| Degree and order 75 | | | 2.1 | $6.1\times10^{-5}$ | .013 |
| 11.0 | 0.111 | 0.19 | 1.90 | $9.7\times10^{-5}$ | .012 |
| 4.1 | .011 | .07 | 1.86 | $6.1\times10^{-5}$ | .012 |
| 2.7 | .036 | .07 | 1.71 | $4.3\times10^{-5}$ | .005 |
| 2.2 | .011 | .05 | 1.63 | $1.3\times10^{-5}$ | .006 |
| 1.83 | .001 | .022 | 1.56 | $7.8\times10^{-6}$ | .001 |
| 1.53 | .005 | .009 | 1.52 | $3.0\times10^{-6}$ | .001 |
| 1.21 | .0001 | .004 | 1.47 | $8.3\times10^{-6}$ | .004 |
| | | | 1.41 | $3.2\times10^{-6}$ | .004 |
| | | | 1.36 | $0.8\times10^{-6}$ | .0004 |
| | | | 1.32 | $2.4\times10^{-6}$ | .003 |
| | | | 1.29 | $1.1\times10^{-6}$ | .002 |
| | | | 1.25 | $2.0\times10^{-6}$ | .001 |
| | | | 1.21 | $0.2\times10^{-6}$ | .002 |
| | | | 1.12 | $3.2\times10^{-11}$ | .0008 |
| | | | 1.07 | $7.2\times10^{-11}$ | .0002 |
| | | | 1.03 | $3.2\times10^{-10}$ | .0006 |

TABLE 11.—*These data correspond to the right side of table 10, but are for the* $N_{11}$ *component.*

| Period (minutes) | MEM Peak $P_{100}$ (EU)$^2$ | Amplitude (EU) |
|---|---|---|
| 91.4 | 562.1 | 7.13 |
| 45.0 | 307.6 | 3.73 |
| 12.5 | .0006 | .26 |
| 10.2 | .0011 | .17 |
| 7.30 | .0032 | .06 |
| 6.19 | $9.1 \times 10^{-4}$ | .23 |
| 4.62 | $3.07 \times 10^{-4}$ | .08 |
| 4.13 | $6.97 \times 10^{-4}$ | .13 |
| 3.60 | $0.81 \times 10^{-4}$ | .10 |
| 3.30 | $1.76 \times 10^{-4}$ | .06 |
| 2.94 | $1.05 \times 10^{-4}$ | .07 |
| 2.80 | $0.53 \times 10^{-4}$ | .09 |
| 2.41 | $.46 \times 10^{-4}$ | .07 |
| 2.25 | $.11 \times 10^{-4}$ | .07 |
| 2.08 | $.91 \times 10^{-4}$ | .05 |
| 1.99 | $.38 \times 10^{-4}$ | .07 |
| 1.87 | $.14 \times 10^{-4}$ | .05 |
| 1.75 | $.20 \times 10^{-4}$ | .05 |
| 1.63 | $4.4 \times 10^{-6}$ | .04 |
| 1.51 | $5.9 \times 10^{-6}$ | .04 |
| 1.45 | $.88 \times 10^{-6}$ | .04 |
| 1.37 | $.55 \times 10^{-6}$ | .03 |
| 1.30 | $.31 \times 10^{-6}$ | .04 |
| 1.26 | $.24 \times 10^{-6}$ | .03 |
| 1.19 | $6.7 \times 10^{-9}$ | .04 |
| 1.02 | $1.9 \times 10^{-11}$ | .04 |



U. S. GOVERNMENT PRINTING OFFICE : 1973 O - 506-579

(Continued from inside front cover)

## NOAA TECHNICAL REPORTS

NOS 41 A User's Guide to a Computer Program for Harmonic Analysis of Data at Tidal Frequencies. R. E. Dennis and E. E. Long, July 1971. Price $0.65 (COM-71-50606)

NOS 42 Computational Procedures for the Determination of a Simple Layer Model of the Geopotential From Doppler Observations. Bertold U. Witte, April 1971. Price $0.65 (COM-71-50400)

NOS 43 Phase Correction for Sun-Reflecting Spherical Satellite. Erwin Schmid, August 1971. Price $0.25 (COM-72-50080)

NOS 44 The Determination of Focal Mechanisms Using P- and S-Wave Data. William H. Dillinger, Allen J. Pope, and Samuel T. Harding, July 1971. Price $0.60 (COM-71-50392)

NOS 45 Pacific SEAMAP 1961-70 Data for Area 15524-10: Longitude 155°W to 165°W, Latitude 24°N to 30°N, Bathymetry, Magnetics, and Gravity. J. J. Dowling, E. F. Chiburis, P. Dehlinger, and M. J. Yellin, January 1972. Price $3.50 (COM-72-51029)

NOS 46 Pacific SEAMAP 1961-70 Data for Area 15530-10: Longitude 155°W to 165°W, Latitude 30°N to 36°N, Bathymetry, Magnetics, and Gravity. J. J. Dowling, E. F. Chiburis, P. Dehlinger, and M. J. Yellin, January 1972. Price $3.50

NOS 47 Pacific SEAMAP 1961-70 Data for Area 15248-14: Longitude 152°W to 166°W, Latitude 48°N to 54°N, Bathymetry, Magnetics, and Gravity. J. J. Dowling, E. F. Chiburis, P. Dehlinger, and M. J. Yellin, April 1972. Price $3.50 (COM-72-51030)

NOS 48 Pacific SEAMAP 1961-70 Data for Area 16648-14: Longitude 166°W to 180°W, Latitude 48°N to 54°N, Bathymetry, Magnetics, and Gravity. J. J. Dowling, E. F. Chiburis, P. Dehlinger, and M. J. Yellin, April 1972. Price $3.00 (COM-72-51028)

NOS 49 Pacific SEAMAP 1961-70 Data for Areas 16530-10 and 17530-10: Longitude 165°W to 180°W, Latitude 30°N to 36°N, Bathymetry, Magnetics, and Gravity. E. F. Chiburis, J. J. Dowling, P. Dehlinger, and M. J. Yellin, July 1972. Price $4.75

NOS 50 Pacific SEAMAP 1961-70 Data for Areas 16524-10 and 17524-10: Longitude 165°W to 180°W, Latitude 24°N to 30°N, Bathymetry, Magnetics, and Gravity. E. F. Chiburis, J. J. Dowling, P. Dehlinger, and M. J. Yellin, July 1972. Price $5.75

NOS 51 Pacific SEAMAP 1961-70 Data for Areas 15636-12, 15642-12, 16836-12, and 16842-12; longitude 156°W to 180°W, Latitude 26°N to 48°N, Bathymetry, Magnetics, and Gravity. E. F. Chiburis, J. J. Dowling, P. Dehlinger, and M. J. Yellin, July 1972. Price $11.00 (COM-73-50280)

NOS 52 Pacific SEAMAP 1961-70 Data Evaluation Summary. P. Dehlinger, E. F. Chiburis, and J. J. Dowling, July 1972. Price $0.40

NOS 53 Grid Calibration by Coordinate Transfer. Lawrence W. Fritz, November 1972. (COM-73-50240)

NOS 54 A Cross-Coupling Computer for the Oceanographer's Askania Gravity Meter. Carl A. Pearson and Thomas E. Brown, November 1972.

NOS 55 A Mathematical Model for the Simulation of a Photogrammetric Camera Using Stellar Control. Chester C Slama, December 1972.

NOS 56 Cholesky Factorization and Matrix Inversion. Erwin Schmid, March 1973.

NOS 57 Complete Comparator Calibration. Lawrence W. Fritz, in press, 1973.

NOS 58 Telemetering Hydrographic Tide Gauge. Charles W. Iseley, in press, 1973.